

## EVAPORATION CONTROLLED EMISSION IN VENTILATED ROOMS

C. Topp, P.V. Nielsen, P. Heiselberg

Department of Building Technology and Structural Engineering, Aalborg University, Denmark

### ABSTRACT

Emission of volatile organic compounds (VOCs) from materials is traditionally determined from tests carried out in small-scale test chambers. However, a difference in scale may lead to a difference in the measured emission rate in a small-scale test chamber and the actual emission rate in a full-scale ventilated room when the emission is fully or partly evaporation controlled. The objective of the present research work has been to investigate the change of emission rates from small-scale experiments to full-scale ventilated rooms and to investigate the influence of the local air velocity field near the source. A series of CFD experiments has been carried out for different set-ups and different air change rates. The results provide a method to compare mass transfer coefficients found in different scales and different geometries for evaporation controlled emission processes. Furthermore, the results show that for a given set-up the mass transfer coefficient increases with velocity and turbulence intensity.

### INTRODUCTION

Traditionally, emission from surfaces is characterized as emission controlled by diffusion through the material or emission controlled by evaporation from the surface. The emission from a material is often determined from tests carried out in a small-scale test chamber. For a given pollutant a difference in scale may lead to a difference in the emission rate measured in the test chamber when the emission is controlled by evaporation and depends on environmental parameters such as temperature, pollutant concentration, humidity, air flow pattern, air velocity and turbulence. This paper deals with evaporation controlled emission influenced by the air flow pattern near the source.

It is assumed that emission of volatile organic compounds (VOCs) from a surface is limited by molecular diffusion through the boundary layer at the surface-air interface see figure 1, and can be described by Fick's law (equation 1). The driving force for the emission from a surface is the difference in concentration between the surface and the air.

$$E = -D \frac{\partial c}{\partial y} \quad (1)$$

$$E = k_c (c_s - c_\infty) \quad (2)$$

$$k_c = \frac{D}{\delta_D} \quad (3)$$

where  $E$ =emission rate ( $\text{mg}/\text{sm}^2$ ),  $D$ =molecular diffusion coefficient ( $\text{m}^2/\text{s}$ ),  $c$ =concentration,  $k_c$ =mass transfer coefficient ( $\text{m}/\text{s}$ ),  $c_s$ =concentration at surface ( $\text{mg}/\text{m}^3$ ),  $c_\infty$ =background concentration ( $\text{mg}/\text{m}^3$ ),  $\delta_D$ =thickness of diffusion boundary layer ( $\text{m}$ ).

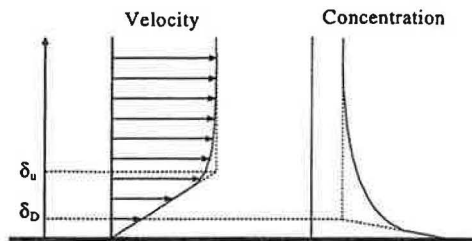


**Figure 1** Velocity and concentration profiles in the turbulent boundary layer.  $\delta_u$  and  $\delta_D$  are the thickness of the velocity and diffusion boundary layer, respectively.

Analogous to heat transfer the emission can be expressed in terms of a mass transfer coefficient,  $k_c$  (equation 2), where  $k_c$  is defined as the molecular diffusion coefficient,  $D$ , divided by the thickness of the diffusion boundary layer,  $\delta_D$  (equation 3).

The thickness of the diffusion boundary layer,  $\delta_D$ , depends on the conditions in the air flow near the source such as velocity and turbulence intensity. Consequently, the thickness of the diffusion boundary layer must be accounted for when describing the emission from a surface. This has been done by Tichenor et al. for small-scale test chambers and large rooms (1). It has been the objective of the present research work to provide a tool that links emission rates found in a small-scale test chamber and in a full-scale ventilated room. A model that expresses the mass transfer coefficient in terms of the air velocity near the surface has been developed for different geometries and different source locations, i.e. different local air flow patterns.

#### METHODS

A series of numerical experiments made by Computational Fluid Dynamics (CFD) has been carried out for a small-scale test chamber and a full-scale ventilated room including different source locations as well as different geometries. The full-scale room is chosen similar to the room used in the International Energy Agency, Annex 20 programme (3) and the different set-ups are shown in Figure 2. Here, the emitting surface is located either at the ceiling or at the floor. To avoid disturbances from inlet conditions and reattachment to the floor an area of 3 m from the inlet or the outlet respectively is not emitting.

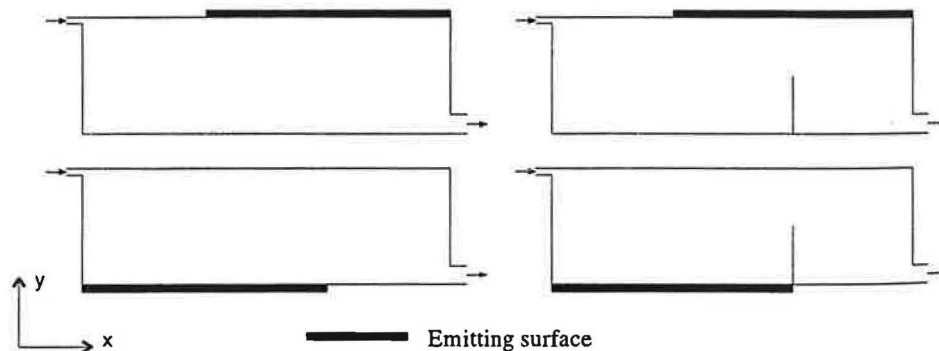


**Figure 2** Outline of the four different set-ups in a test room with two-dimensional flow (3). In two of the cases a wall (height 1.5 m) is located at  $x = 6$  m. The length of the room is 9 m, the height of the room is 3 m, the height of the inlet is 0.168 m and the height of the outlet is 0.48 m.

The test chamber is chosen as two emitting surfaces with typical length and spacing as used in the CLIMPAQ unit (2), see Figure 3.

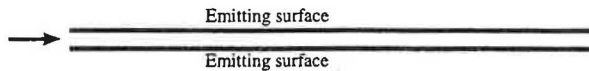


Figure 3 The length of the test chamber is 0.8 m and the distance between the two emitting surfaces is 0.02 m (2).

In all cases a hypothetical source is used. The concentration at the surface is  $c_s = 1000 \text{ mg/m}^3$  and the molecular diffusion coefficient is  $D = 15.1 \cdot 10^{-5} \text{ m}^2/\text{s}$ .

Usually, the  $k$ - $\epsilon$  turbulence model, where  $k$  is the turbulent kinetic energy and  $\epsilon$  is the dissipation of energy, is used to calculate room air flow (4). The model is based on the assumption that the flow is fully turbulent which is not true in the near wall region where the local Reynolds number is so small that the transport equations for the turbulent quantities,  $k$  and  $\epsilon$ , do not apply. When modelling flow in the wall region the problem can be accounted for either by adding molecular diffusion terms to the  $k$ - $\epsilon$  model (Low Reynolds Number model, LRN model) or by using a wall function (4). In terms of computational time the LRN model is expensive because it requires a high resolution of the boundary layer. The wall function describes the profile close to the wall and connects the wall boundary conditions with the properties in the fully turbulent layer. Consequently, grid points are not needed in that region. In the present case the interest is focused on the near wall region and the LRN model is therefore used.

## RESULTS

The results from the CFD experiments are evaluated at  $x = 3 \text{ m}$  for the floor and at  $x = 6 \text{ m}$  for the ceiling. To investigate the influence of the velocity field near the source of emission a reference velocity is required. The reference velocity used for the test room is the local maximum velocity,  $u_{\text{max}}$ , in the  $x$ -direction and for the test chamber the inlet velocity is used. Typical velocity profiles from the test room are shown in figures 4 and 5.

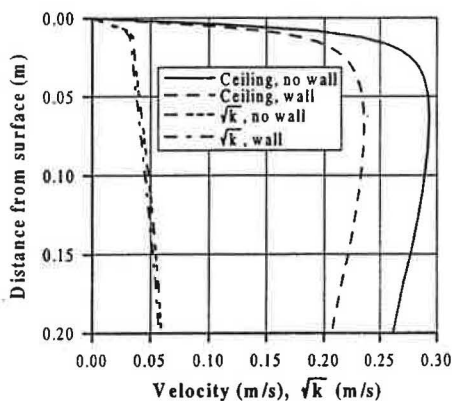


Figure 4 Velocity profiles and turbulence levels at the ceiling in the two-dimensional test room at  $x=6\text{m}$  and an air change rate of  $10 \text{ h}^{-1}$ .

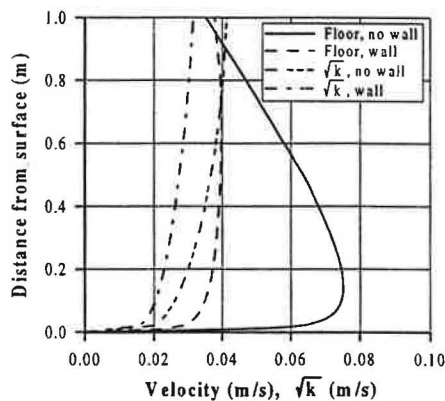


Figure 5 Velocity profiles and turbulence levels at the floor in the two-dimensional test room at  $x=3\text{m}$  and an air change rate of  $10 \text{ h}^{-1}$ .

In mixing ventilation the recirculating flow is similar to a wall jet and the level of turbulence can be expressed by  $\sqrt{k} \approx 1.1RMS$  where  $k$  is the turbulent kinetic energy and  $RMS$  is the Root Mean Square value of the velocity fluctuations in the flow direction (5). The parameter  $\sqrt{k}$  has been included in the figures to illustrate the level of turbulence. Both at the ceiling and at the floor the velocity is reduced by the wall but the level of turbulence is increased.

Figures 6 and 7 show typical concentration profiles in the two-dimensional test room. Close to the wall in the laminar part of the boundary layer, the emission is controlled by molecular diffusion due to the concentration gradient. At the ceiling the concentration gradient is steeper than at the floor due to the higher velocity.

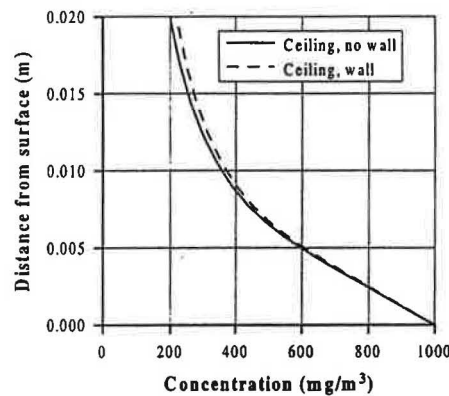


Figure 6 Concentration profiles at the ceiling in the two-dimensional test room at  $x=6$  m and an air change rate of  $10 \text{ h}^{-1}$ .

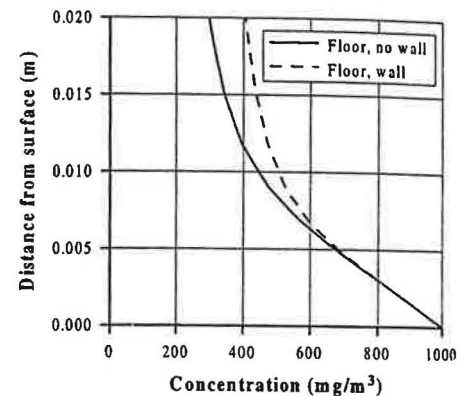


Figure 7 Concentration profiles at the floor in the two-dimensional test room at  $x=3$  m and an air change rate of  $10 \text{ h}^{-1}$ .

The concentration distributions are also outlined in figure 8 together with the flow field. It can be seen that the free wall affects the flow field and, consequently, the concentration distribution. The larger influence from the wall occurs when the emission source is located at the floor.

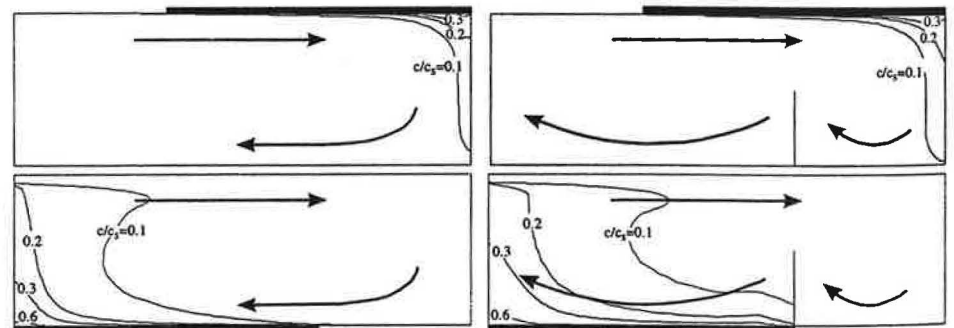


Figure 8 Concentration distributions in the two-dimensional test room for the four different set-ups corresponding to an air change rate of  $10 \text{ h}^{-1}$ .

The mass transfer coefficient,  $k_c$ , is obtained from equation 2 with the emission rate,  $E$ , the surface concentration,  $c_s$ , and the background concentration,  $c_\infty$ , as input.  $E$  and  $c_s$  are fixed but  $c_\infty$  is not well defined. In the present case the local concentration at  $y = 1.5$  m has been chosen as the background concentration. In figure 9 the relation between the reference velocity and the mass transfer coefficient,  $k_c$ , is shown for the 4 set-ups as well as for the CLIMPAQ unit for different air change rates.

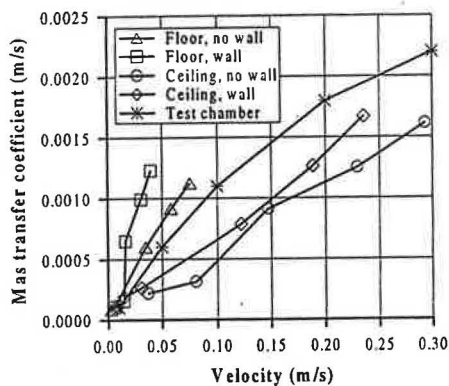


Figure 9 Relation between mass transfer coefficient and velocity based on the local background concentration at  $y=1.5$  m for different air change rates.

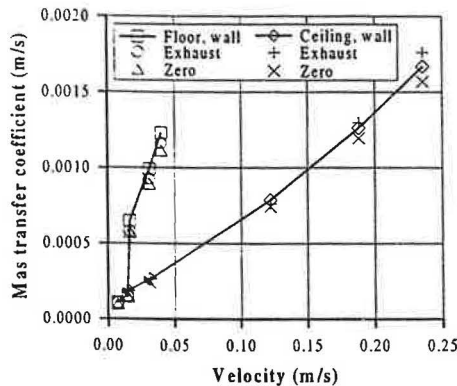


Figure 10 Examples of the relation between mass transfer coefficient and velocity based on different definitions of the background concentration.

Two other definitions of the background concentration based on different assumptions have been investigated. If the VOCs in the room were fully mixed which they are not in the present case, the background concentration,  $c_\infty$ , would be defined as the concentration in the exhaust air. Another way of handling  $c_\infty$  is to neglect the term but this is not correct according to the concentration profiles. The influence of the background concentration is illustrated in figure 10 where the relation between the mass transfer coefficient and the reference velocity is shown for the three definitions of the background concentration.

## DISCUSSION

The influence of local air flow conditions on the molecular diffusion through a laminar boundary layer has been investigated. It is shown that velocity, turbulence and background concentration, due to different geometries give highly different mass transfer coefficients at a given velocity. Consequently, when testing a material in a small-scale test chamber the air velocity should not be the expected velocity in a full-scale ventilated room. If, in the present case,  $u_{\max} = 0.15$  m/s at the ceiling in the empty room the material should be tested at 0.08 m/s in the test chamber to obtain the actual mass transfer coefficient at  $k_c = 0.0009$  m/s. Furthermore, the CFD experiments show that for a specific set-up the mass transfer coefficient increases with velocity and turbulence.

At a given air change rate the velocity levels at the floor and the ceiling respectively, are much different but the difference in mass transfer coefficient is not as significant. This is due to the higher turbulence level at the floor.

The background concentration,  $c_{\infty}$ , also influences the mass transfer coefficient and three definitions of  $c_{\infty}$  have been investigated. Defining  $c_{\infty}$  as the concentration in the exhaust air is based on the assumption that the VOCs in the room are fully mixed which is rarely the situation. Another way of handling the background concentration is to neglect the influence and let  $c_{\infty} = 0$  which is not true either. Here, the local background concentration at  $y=1.5\text{m}$  has been used.

When the floor is emitting, the source is located far from the outlet and the local background concentration is higher than the concentration in the exhaust air. Therefore, the mass transfer coefficient based on the local background concentration is the higher one. The deviation from the mass transfer coefficient based on the local background condition is 0-10 % if  $c_{\infty}$  is based on the concentration in the exhaust air and 5-15 % if  $c_{\infty}$  is neglected.

If the source is located at the ceiling, it is closer to the outlet and the order of the concentrations are reversed. Consequently, the mass transfer coefficient based on the concentration in the exhaust air is the higher one. In this case the deviation from the mass transfer coefficient based on the local background condition will be 0-5 % if  $c_{\infty}$  is based on the concentration in the exhaust air and 0-10 % if  $c_{\infty}$  is neglected.

#### ACKNOWLEDGEMENTS

This research work has been supported financially by the Danish Technical Research Council (STVF) as a part of the research programme "Healthy Buildings".

#### REFERENCES

1. Tichenor, B.A.; Guo, Z. and Sparks, L.E. 1993. "Fundamental Mass Transfer Model for Indoor Air Emissions from Surface Coatings." *Indoor Air 1993*. Vol. 3, pp. 263-268.
2. Gunnarsen, L.; Nielsen, P.A. and Wolkoff, P. 1994. "Design and Characterization of the CLIMPAQ, Chamber for Laboratory Investigations of Materials, Pollution and Air Quality." *Indoor Air 1994*. Vol. 4, pp. 56-62.
3. Nielsen, P.V. 1990. "Specification of a Two-Dimensional Test Case." Internal Report for the International Energy Agency, Annex 20, Aalborg University Denmark.
4. Launder, B.E. and Spalding, D.B. 1974. "The Numerical Computation of turbulent Flows." *Computer Methods in Applied Mechanics and Engineering*. Vol. 3, pp. 269-289.
5. Nielsen, P.V. 1989. "Airflow Simulations Techniques - Progress and Trends." *Proceedings of the 10th AIVC Conference*, Espoo, Finland.
6. Nielsen, P.V. 1995. "Healthy Buildings and Air Distribution in Rooms." *Proceedings of Healthy Buildings '95*, Milan (Italy), Vol. 2, pp. 923-928.